UAV Sensor Orientation with Pre-calibrated Redundant IMU/GNSS Observations: Preliminary Results

PHILIPP CLAUSEN[1], MARTIN REHAK[1] & JAN SKALOUD[1]

Zusammenfassung: In unserem Beitrag stellen wir eine Drohne vor, welche für eine hochpräzise Kartographie mit Positions- und Orientierungssensoren ausgestattet ist. Der Einsatz der Sensoren als absolute und relative Messung kann die Genauigkeit des Mappings erhöhen, falls die Sensoren korrekt kalibriert sind. Dies zeigen wir an einem Fallbeispiel, in dem eine Blockstruktur beflogen wurde, in welcher Passpunkte (Ground Control Points) nur lokal angelegt wurden. Eine redundante Sensor-Konfiguration zeigt dann auf, wie gut und genau die Kalibrierung und dessen Resultat sind.

1 Introduction

1.1 General Concepts

Unmanned aerial vehicles (UAVs) are an important tool for surveyors, construction engineers and scientists worldwide. Thanks to their affordability and recent advances in guidance, autonomy, and easiness of use, they spread among wide public. Accurate georeferencing plays a key role in successful terrain reconstruction and artefact-free orthophoto generation; it is particularly of great relevance in applications such as corridor mapping, road and pipeline inspections, and mapping of large areas with homogeneous surface structure, e.g. forests or agricultural fields.

The presented experiments focus on new approaches of aerial control. The accuracy in the aforementioned mapping scenarios can be quantitatively improved by new approaches of aerial position and relative attitude control. By differencing the observations, the process of system calibration is simplified and some of the systematic errors in the observations are ruled out. This is interesting in the context of mapping with micro aerial vehicles (MAVs) that have limited payload capacity and flight endurance. The asset of aerial relative control is further increased by using redundant attitude observations.

1.2 Challenge

We investigate the proposed methods of georeferencing on a real data set acquired with a custom-built MAV fixed-wing plane. It is equipped with a geodetic-grade GNSS receiver and a redundant Inertial Measurement Unit (R-IMU) that is based on Micro-Electro-Mechanical-Systems (MEMS). This R-IMU was specifically developed to be employed on MAVs. To achieve accurate results, a state-of-the-art sensor calibration is presented here and performed. This procedure estimates the deterministic errors present in the sensors. The camera system is pre-calibrated for the lens-distortions, whereas a self-calibration is performed for the principal point and the distance. We show methods of handling the redundant observations. First, several independent sets of exterior orientation (EO) parameters are calculated and then used in a Bundle Block Adjustment

---

[1] École Polytechnique Fédérale de Lausanne, CH-1015 Lausanne, Switzerland, E-Mail: {philipp.clausen, martin.rehak, jan.skaloud}@epfl.ch

(BBA). These observation are treated in an absolute and relative manner, giving raise to different solutions.

We evaluate the proposed calibration and orientation methods during a real mapping project. The accuracy of the mapping solution is assessed via a set of independent check points that were accurately surveyed. We confirm that thanks to on-board observations of UAV-position and attitude a centimetre mapping accuracy is achievable using proper pre-calibration and processing techniques in scenarios where classical methods of sensor orientation fail (i.e. deliver non-acceptable lower accuracy by a factor superior to 10).

1.3 Paper Structure

The photogrammetric system used on the MAV is described in Section 2. Section 3 details the inertial navigation system with its calibration and properties. Section 4 introduces the custom-built MAV and the dataset we collected with it. The final results are reported and discussed in Section 5. The conclusion in Section 6 then rounds up the paper.

2 Photogrammetric System

The imaging system is composed of the Sony NEX 5R camera with a 16 mm Sony lens. It is mounted next to the in-house developed GECKO4Nav-Board (KLUTER 2012), which is shown in Figure 1. The specifications of the installed IMUs are explained in detail in Section 3. The IMUs and the camera system are rigidly mounted so that their relative orientation stays the same over the whole period of testing. This is assured by the means of a stable carbon structure.
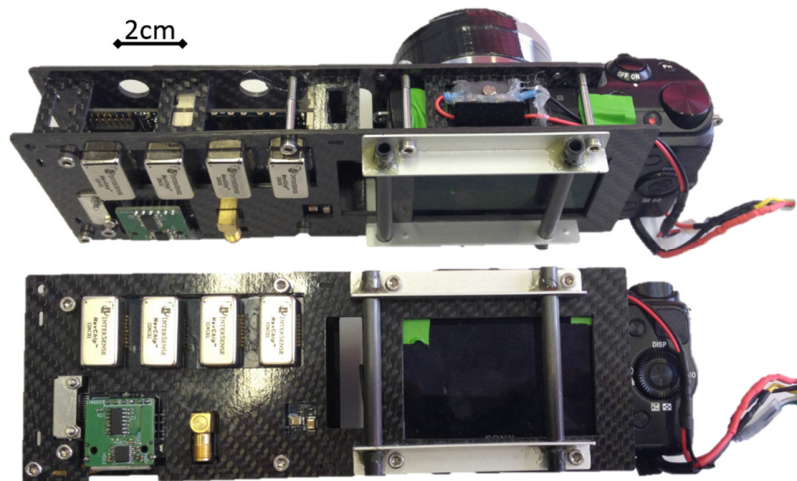

Fig. 1:   GECKO4Nav-Board on the left side and the Sony Camera on the right side rigidly connected through a carbon structure.

Precise timestamping of the IMUs to the GPS-time is assured by a geodetic grade GNSS receiver, which is directly connected to the GECKO4Nav-Board. The PPS signal serves as synchronization among all the components. It synchronizes the individual IMUs to the common clock. The camera is synchronized to the GNSS receiver by sending a pulse every time the shutter opens. Thus, the

exact time of each picture is very well known. The weight of the photogrammetric payload shown in Figure 1 is around 550 g.

The IMUs mounted next to the photogrammetric system are MEMS-IMUs with an interesting noise characteristics (INTERSENSE 2015). The most pertinent error-characteristics are shown in Table 1. The increased noise characteristics (in comparison to a tactical grade IMU) are compensated with their weight of only 6 g. This makes them perfectly usable in MAVs, although some electronics have to be designed for synchronization, timestamping, and power control.

Tab. 1: Properties of one Navchip-IMU.

Property	Value
size	24x14x9 mm
weight	6 g
power requirement	0.2 W
frequency	250 Hz
gyro bias	10 °/hr

3   Redundant IMU

There are several advantages of using multiple IMUs at the same time (GUERRIER et al. 2012). One of the advantages is *redundancy*: if one sensor fails or delivers faulty observations, then the other sensor can detect it and compensate the error. Another advantage is related to the value of the noise level. By combining multiple sensors in a *synthetic* IMU the overall noise is first determined and then reduced (WAEGLI et al. 2010). This is advantageous, as the noise-level may vary due to vibrations and its exact value is required for the filtering/smoothing with GNSS data. Before using the R-IMU concept the sensors have to be calibrated for deterministic errors.

A total number of four Navchip-IMUs are mounted next to each other (Figure 1). The IMU-sensor-system is placed at different attitudes where static measurements l are taken for several seconds. The amplitude $\|l\|$ is compared to the reference gravity signal $\|g\|$ taking advantage of the compensation process explained by Syed et al. (SYED et al. 2007). The bias b, the mean scale factor S, and the non-orthogonality θ between the individual sensor axes x, y and z can be estimated. The found properties are then applied to compensate the measurements of the accelerometers l according to the formula:

$$\begin{pmatrix} l_x \\ l_y \\ l_z \end{pmatrix}_{compensated} = \begin{bmatrix} 1+S_x & 0 & 0 \\ \theta_{xy} & 1+S_y & 0 \\ \theta_{xz} & \theta_{yz} & 1+S_z \end{bmatrix} \begin{pmatrix} l_x \\ l_y \\ l_z \end{pmatrix} + \begin{pmatrix} b_x \\ b_y \\ b_z \end{pmatrix} \tag{1}$$

Figure 2 shows the norm of the accelerometer measurements before and after calibration for one IMU. The wrong norm in different positions is due to the fact that each axis has an individual bias, and that the axis are coupled through the non-orthogonality. The corrected signal can then be used in the next processing steps explained in the following subsection. These procedure of calibration is used separately on the four IMUs.
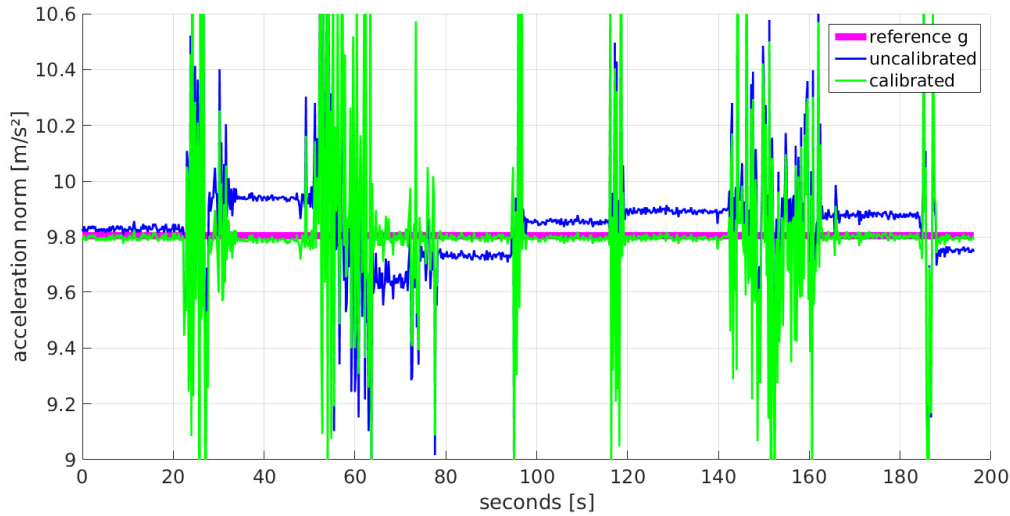
Fig. 2: Example dataset before (blue) and after (green) calibration of an IMU showing the differences in the acceleration norm at different attitudes. The reference gravity value g is shown in red colour.

The resulting biases from the calibration process are shown in Table 2, where one can see that each IMU has its own error characteristics. Therefore, a thorough calibration is an absolute necessity for each sensor as the results are not similar at all. Wrongly calibrated accelerometer sensors can for instance lead to wrong attitude determination.

Tab. 2: Sensor error bias example is shown for all four IMUs.

Property	IMU 0	IMU 1	IMU 2	IMU 3
b_x [µg]	6764	5945	11397	-997
b_y [µg]	16225	4198	1538	28220
b_z [µg]	-871	-2507	-2058	-5372

4 MAV Platform and Test Data

4.1 MAV Platform

A custom-developed MAV platform was used to collect data for this study. The fixed-wing platform has a wingspan of 1630 mm and a length of 1170 mm. The maximal payload capacity is around 800 g. The operational weight varies between 2200-2800 g. The aircraft is made of expanded polypropylene foam (Figure 3). The flexible nature of the construction material makes the platform resistant to damage. The plane is easy to assemble and repair with ordinary hobby-grade tools. The cost of the system components is significantly lower with respect to size and endurance compared with other platforms (MAVINCI 2015). The endurance with 600 g payload is approximately 40 minutes. The plane is controlled by a Pixhawk autopilot that has been intensively developed over the last few years (MEIER et al. 2012).
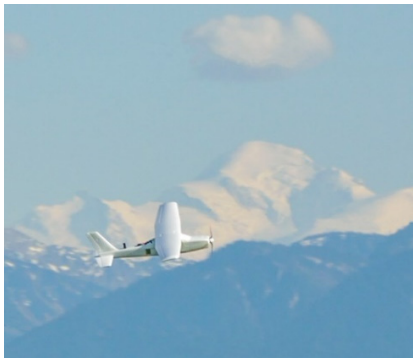
Fig. 3:   Custom-built MAV platform flying.

Tab. 3: Summary of acquired data for the flight of Figure 4.

Property	Value
camera	Sony Nex 5R
lens	Sony 16 mm
flying height	120-150 m
mean GSD	4.5 cm/pix
overlap forward/lateral	80-60 %
number of Photos	207
number of GCPs	5
number of ChPs	15

4.2   Test data

This study was conducted over agricultural fields and roads. The testing area has a size of approximately 70 ha and is equipped with 20 permanent markers whose location is accurately surveyed. Regarding the accuracy assessment, 15 points were used as independent Check-Points (ChPs) and 5 points were used as ground-control-points (GCPs). The GCPs cover only 1/3 of the area. This is done to simulate a case where the majority of the mapping-area is badly accessible. The data set contains data from a block consisting of 7 parallel lines and 7 lines perpendicular to them, flown in two separate flight heights (Figure 4). This separation is important when performing camera self-calibration since it helps with decorrelating internal and external camera parameters. The most pertinent facts about the flown mission are summarized in Table 3.
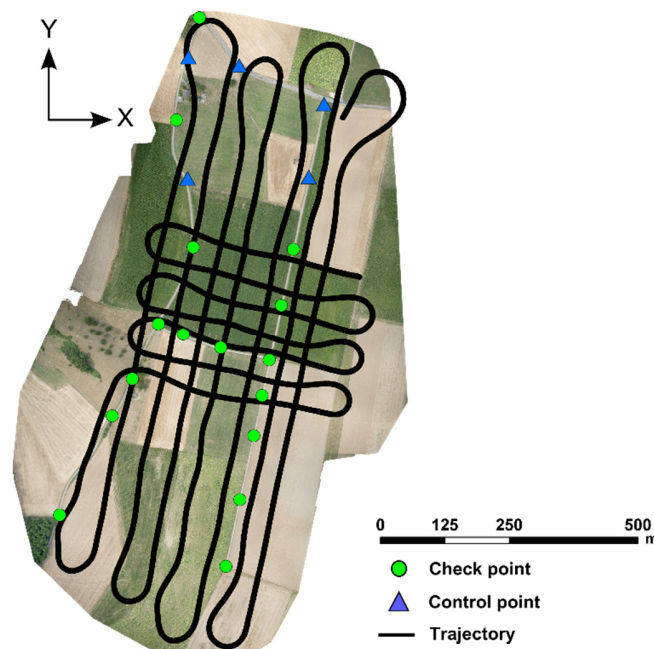

Fig. 4:   Flown mission in Vufflens, Switzerland in 2015. The GCPs (blue triangles) are "badly" placed in order to simulate inaccessible area for GCPs. The black flight line shows the perpendicular flying path at two different heights.

4.3 Processing strategy

The data recorded during the flights were pre-processed in a way similar to mature mapping systems. The GNSS data was processed in a professional software package. Thanks to the precise time synchronization between the camera and the GNSS receiver, the exact acquisition time of each image is directly known. The calculated antenna positions were subsequently fused in an Extended Kalman filter with the IMU at a frequency of 250 Hz. The GNSS/INS-derived attitude was then corrected for the boresight misalignment, which was calibrated in previous experiments (REHAK & SKALOUD 2015). Nevertheless, the inclusion of relative attitude eliminates the need of such calibration. The image observations of the tie-points were automatically measured in the images using Pix4D mapper (PIX4D 2015). The observations of GCPs and ChP were obtained manually using its rayCloud engine.

The observations were then processed in a custom-developed Bundle Block Adjustment (BBA) software. The latter was developed because the offer of commercially available software for BBA allowing redundant and relative position and attitude observations is very limited. In addition, custom implementation gives us full control of observation stochastic modelling that is important when using accurate aerial control. Several BBA projects were created with different inputs.

5 Assessment of Approach: Redundancy in EO observations

Redundancy of EO parameters is very interesting with MAVs. Particularly of interest is the concept of relative orientation as it eliminates the need for boresight calibration of each sensor and decreases the noise level of the whole system. The redundancy in IMU data can be treated in several ways. A first option is the joint utilization of several IMUs as explained by WAEGLI et al. (2008). The second option is based on computing several trajectories and inputting them as additional observations into the BBA. However, the introduction of absolute attitude control would require separate boresight calibration of all IMUs as well as handling the correlations among them. Here, the relative orientation has a big potential since the boresights are eliminated and the residual correlations become very small. Several BBA projects were computed with different inputs and kinds of aerial control. The first test includes the following projects using always 5 GCPs:

(1) Indirect Sensor Orientation (SO)
(2) Integrated SO (ISO) with *un*calibrated IMU using absolute position and attitude
(3) ISO with *pre*calibrated IMU using absolute position (Ap) and absolute attitude (Aa)
(4) ISO with *pre*calibrated IMU using absolute position (Ap) but relative attitude (Ra)

The results of this first test is given in Table 4. The Indirect SO solution (1) can be massively improved by using the absolute position and absolute attitude of the camera system (2). This solution (2) is using the uncalibrated IMU and can then be further improved by utilizing the precalibrated IMU (3). The RMS value decreases slightly for the Z-axis. However, the impact would be larger for situations with fewer image observations. The results in the Z-axis can be improved even further by employing the approach (4) with the relative attitude update. This test evidences the influence of the calibrated IMU data on the relative attitude updates. Detailed investigations on relative attitude observations are presented in REHAK & SKALOUD (2016).

Tab. 4: Accuracy assessment at independent ChPs. The block has 5 GCPs and 15 ChPs. The IMU number "0" was used with absolute position (Ap), absolute attitude (Aa), and relative attitude (Ra).

Dataset	Accuracy					
	Mean ChP [mm] | [px]			RMS ChP [mm] | [px]		
	X	Y	Z	X	Y	Z
(1) Indirect SO	68 | 1.5	8 | 0.2	-664 | 14.8	16 | 0.4	145 | 3.2	1171 | 26
(2) ISO Ap Aa *uncalib*	13 | 0.3	26 | 0.6	74 | 1.6	26 | 0.6	37 | 0.8	87 | 1.9
(3) ISO Ap Aa *precalib*	14 | 0.3	25 | 0.6	64 | 1.4	28 | 0.6	35 | 0.8	78 | 1.7
(4) ISO Ap *R*a precalib	14 | 0.3	24 | 0.5	45 | 1.0	27 | 0.6	36 | 0.8	65 | 1.4

The second test was conducted to verify if the IMU calibration combined with the subsequent use of attitude updates is consistent on all four IMUs of the Gecko4Nav-Board. The following tests were made:

(1) ISO with precalibrated IMU 0 using absolute position (Ap) and absolute attitude (Aa)
(2) ISO with precalibrated IMU 1 using absolute position (Ap) and absolute attitude (Aa)
(3) ISO with precalibrated IMU 2 using absolute position (Ap) and absolute attitude (Aa)
(4) ISO with precalibrated IMU 3 using absolute position (Ap) and absolute attitude (Aa)

The results are provided in Table 5. The results are all similar in the horizontal axes (around 0.6 px in X and 0.8 px in Y). Larger variations in the RMS are present in Z-direction (1.6 px to 2.2 px) among individual solutions. In comparison to indirect SO (that has around 26 px) the improvement factor is around 10. Small differences can arise from the Kalman Filter solution, since the same stochastic model has been used for each of the IMUs.

Tab. 5: Accuracy assessment at independent ChPs. The block has 5 GCPs and 15 ChPs. All precalibrated IMUs "0" to "3" were used with absolute position (Ap) and absolute attitude (Aa).

Dataset	Accuracy					
	Mean ChP [mm] | [px]			RMS ChP [mm] | [px]		
	X	Y	Z	X	Y	Z
(1) ISO Ap Aa IMU *0*	14 | 0.3	25 | 0.6	64 | 1.4	28 | 0.6	35 | 0.8	78 | 1.7
(2) ISO Ap Aa IMU *1*	7 | 0.2	26 | 0.6	85 | 1.9	21 | 0.5	37 | 0.8	98 | 2.2
(3) ISO Ap Aa IMU *2*	8 | 0.2	25 | 0.6	66 | 1.5	26 | 0.6	35 | 0.8	82 | 1.8
(4) ISO Ap Aa IMU *3*	6 | 0.1	27 | 0.6	56 | 1.2	23 | 0.5	37 | 0.8	73 | 1.6

6   Conclusion and perspectives

We presented the advantages of using position and attitude aerial control over the indirect sensor orientation. The importance of attitude increases with a decreasing number of image observations, and it depends on the texture of the mapping area and on an unfavourable image geometry (i.e. low overlap or corridor). The pre-calibration of low-cost IMUs is recommended since it improves the accuracy in the Z-direction. Relative attitude updates mitigate the residual misalignment and eliminate the need for precise boresights between camera and IMU. Depending on the demanded accuracy, areas with difficult access for placing GCPs can be skipped because few GCPs are sufficient in the ISO.

We will further investigate different methods of introducing redundant IMU measurements directly into the BBA.

7   References

GUERRIER, S., WAEGLI, A., SKALOUD, J. & VICTORIA-FESER, M.-P., 2012: Fault detection and isolation in multiple mems-imus configuration. IEEE Transactions on Aerospace and Electronic Systems **48**, 2015-2031.

KLUTER, T., 2012: GECKO4NAV Technical Reference Manual Revision 1.0.

MAVINCI, 2015: MAVinci – Unmanned Aerial Systems. URL http://www.mavinci.de/. Accessed 2015-12-10.

MEIER, L., TANSKANEN, P., HENG, L., LEE, G., FRAUNDORFER, F. & POLLEFEYS, M., 2012: PIXHAWK: A micro aerial vehicle design for autonomous flight using onboard computer vision. Autonomous Robots **33**, 21-39.

INTERSENSE, 2015: Intersense Navchip. URL http://www.intersense.com/pages/16/246/. Accessed 2015-12-10.

PIX4D, 2015: Pix4Dmapper. URL http://pix4d.com/. Accessed 2015-12-10.

REHAK, M. & SKALOUD, J., 2015: Fixed-Wing Micro Aerial Vehicle for Accurate Corridor Mapping. ISPRS Annals of the Photogrammetry, Remote Sensing and Spatial Information Sciences **2** (1/W1), 23-31.

REHAK, M. & SKALOUD, J., 2016: Applicability of new Approaches of Sensor Orientation to Micro Aerial Vehicles. The International Annals of Photogrammetry, Remote Sensing and Spatial Information Sciences ISPRS ICWG III/I Annals of ISPRS Congress, Prague.

SYED, Z.P., AGGARWAL, P., GOODALL, C., NIU, X. & EL-SHEIMY, N., 2007: A new multi-position calibration method for MEMS inertial navigation systems. Measurement Science and Technology **18**, 1897-1907.

WAEGLI, A., GUERRIER, S. & SKALOUD, J., 2008: Redundant MEMS-IMU integrated with GPS for performance assessment in sports. Proceedings of the IEEE/ION PLANS 2008, Monterey, CA, USA.

WAEGLI, A., SKALOUD, J., GUERRIER, S. & PARES, M., 2010: Noise reduction and estimation in multiple micro-electro-mechanical inertial systems. Measurement Science and Technology **21**, 065201-065212.